HHS Public Access

Author manuscript

Reproduction. Author manuscript; available in PMC 2020 October 01.

Persistent effects on bovine granulosa cell transcriptome after resolution of uterine disease

Rachel L. Piersanti[1], **Anthony D. Horlock**[2], **Jeremy Block**[1], **José E.P. Santos**[1], **I. Martin Sheldon**[2], **John J. Bromfield**[1,*]

[1]Department of Animal Sciences, University of Florida, Gainesville 32611.

[2]Institute of Life Science, Swansea University Medical School, Swansea, SA2 8PP, UK.

Abstract

Metritis is associated with reduced fertility in dairy cows, but the mechanisms are unclear because the disease resolves several weeks before insemination. One hypothesis is that metritis causes persistent changes in granulosa cells during follicle development, which might be evident in the transcriptome of granulosa cells from dominant follicles weeks after parturition. To test this hypothesis we collected follicular fluid and granulosa cells from dominant follicles 63 days post partum from cows previously diagnosed with metritis, at least 6 weeks after resolution of the disease, and from cows not diagnosed with metritis (control cows). Bacterial lipopolysaccharide was detected in follicular fluid, and concentrations were associated with follicular fluid IL-8 and glucose concentrations. Transcriptome analysis using RNAseq revealed 177 differentially expressed genes in granulosa cells collected from cows that had metritis compared with control cows. The most upregulated genes were *ITLN1*, *NCF2*, *CLRN3*, *FSIP2* and *ANKRD17*, and the most downregulated genes were *ACSM1*, *NR4A2*, *GHITM*, *CBARP* and *NR1I3*. Pathway analysis indicated that the differentially expressed genes were involved with immune function, cell-cell communication, cell cycle and cellular metabolism. Predicted upstream regulators of the differentially expressed genes included NFκB, IL-21 and lipopolysaccharide, which are associated with infection and immunity. Our data provide evidence for a persistent effect of metritis on the transcriptome of granulosa cells in ovarian follicles after the resolution of disease.

Keywords

metritis; transcriptome; granulosa cell; inflammation; immunity

INTRODUCTION

Bacterial infections cause metritis in 10 to 20% of dairy cows within 21 days post partum (Huzzey *et al*. 2007, Sheldon *et al*. 2009, LeBlanc *et al*. 2011, Bromfield *et al*. 2018). Metritis is important because the disease is associated with reduced conception rates and

[*]**Correspondence to**: John J. Bromfield, PhD, Department of Animal Sciences, University of Florida, Gainesville, Florida, 32611, USA, jbromfield@ufl.edu.

DECLARATION OF INTEREST

The authors have no conflict of interest that could be perceived as prejudicing the impartiality of the research reported.

infertility (Ribeiro *et al*. 2016). However, the mechanisms linking metritis and fertility are unclear because the disease resolves several weeks before animals are inseminated. As each ovulatory dominant follicle takes 120 days to develop from a primordial follicle (Britt *et al*. 2018), one possibility is that metritis causes a persistent change in the granulosa cell transcriptome that impairs ovulatory follicles several weeks after parturition.

Postpartum uterine disease is associated with infection of the uterus with a wide range of Gram-negative and Gram-positive pathogenic bacteria (Sheldon *et al*. 2002, Bicalho *et al*. 2012). The most prevalent pathogenic bacteria associated with uterine disease are *Escherichia coli*, *Trueperella pyogenes*, *Prevotella sp*. and *Fusobacterium sp*. (Sheldon *et al*. 2002, Williams *et al*. 2005, Sheldon *et al*. 2010, Amos *et al*. 2014). Sequencing techniques have further advanced our understanding of the uterine microbiome and bacterial diversity and associations with uterine health and disease (Santos & Bicalho 2012, Jeon *et al*. 2016). These pathogens express multiple pathogen-associated molecular patterns, including lipopolysaccharide (LPS) and lipopeptides, which are sensed by immune cells and endometrial cells (Moresco *et al*. 2011, Turner *et al*. 2014). Activation of innate immunity leads to nuclear translocation of transcription factors, including NFκB, stimulating secretion of cytokines such as interleukin (IL)-1 and IL-6, and chemokines such as IL-8. In addition, the pathogens produce pore-forming toxins that cause cell damage, leading to further pathology in the endometrium (Amos *et al*. 2014). Although the bacteria are confined to the genital tract, infected animals have slower growth of the dominant follicle and altered steroidogenesis during the active disease, and are less likely to ovulate (Sheldon *et al*. 2002, Herath *et al*. 2007). Additionally, LPS is found in the follicular fluid of dairy cows that previously had uterine infection (Herath *et al*. 2007).

Granulosa cells determine follicle growth, steroidogenesis, oocyte development, and ovulation (Canipari 2000, Gioacchini *et al*. 2018), coordinating these events by modulating gene expression throughout development and growth of the follicle (Hatzirodos *et al*. 2014). In vitro, granulosa cells isolated from growing and dominant follicles respond to LPS by producing inflammatory mediators, and reducing estradiol synthesis by downregulating *CYP19A1* expression (Bromfield & Sheldon 2011, Price *et al*. 2013). Additionally, LPS negatively impacts the ability of the oocyte to complete meiosis to metaphase II and subsequently form healthy embryos (Soto *et al*. 2003, Bromfield & Sheldon 2011, Sheldon *et al*. 2014). The phenotypic effects of uterine infection on ovarian function and the capacity of granulosa cells to respond to pathogen-associated molecules imply that the ovary could contribute to reduced fertility after the resolution of metritis. However, it is unclear if the ovary retains a molecular imprint of uterine infection to modulate ovarian function after the clearance of disease.

One hypothesis is that metritis causes persistent changes in granulosa cells during follicle development, which might be evident in the transcriptome of granulosa cells from dominant follicles several weeks after parturition. Here, we used RNA sequencing (RNAseq) of granulosa cells collected from dominant follicles around the expected time of insemination for dairy cows and more than 6 weeks after the resolution of metritis. Compared with control, granulosa cells isolated from cows with metritis had 177 differentially regulated genes, which were associated with 39 canonical pathways, including multiple pathways

linked with immune responses. These data provide evidence that postpartum metritis has a persistent effect on the granulosa cell transcriptome, which could negatively impact oocyte quality, ovarian function, and fertility.

MATERIALS AND METHODS

Ethical statement

Animal procedures were approved by the University of Florida Institutional Animal Care and Use Committee (protocol 201508884).

Study Design and Animal Procedures

The design was a prospective cohort study conducted from June 2016 to February 2017 at the University of Florida Dairy Unit using a group of 45 lactating Holstein *Bos taurus taurus* dairy cows fed a total mixed ration and housed in barns with fans and sprinklers for cow comfort.

Milk yield (AfiFlo milk meters, S.A.E. Afikim, Israel) and concentrations of fat, true protein, and lactose (AfiLab online real-time milk analyzer, S.A.E. Afikim) were recorded at each milking, and cows were weighed on a walk through scale (AfiWeigh, S.A.E. Afikim) immediately after each milking as they left the milking parlor. Data were collected for the first 280 days postpartum or until the cow died or was culled, whichever occurred first.

Cows were evaluated every 48 h for the first 21 days after parturition for signs of metritis as defined by a fetid, red-brown watery vaginal discharge and rectal temperature > 39.5°C (Sheldon *et al.* 2006). Cows with metritis received antimicrobial treatment with 2.2 mg/kg body weight ceftiofur hydrochloride (Excenel, Zoetis, Parsippany, NJ, USA) for 5 consecutive days. The veterinarians and farm staff recorded other diseases diagnosed within 21 d post partum, including mastitis, ketosis, displaced abomasum and lameness. Ketosis was diagnosed by evaluating elevated urine ketones, mastitis was defined as any clinical infection of the udder, displaced abomasum was diagnosed by auditory examination of the abdomen and lameness was defined as cows with any number of foot/hoof conditions impacting ambulatory movement. Cows were examined for clinical endometritis, as determined by a purulent vaginal discharge after d 21 post partum, and for subclinical endometritis, as determined by > 5% neutrophils in endometrial cytology samples collected on the day of follicle aspiration, at 63 days postpartum. Cows with post partum conditions beyond 21 days after parturition were excluded from analysis.

Cows started a an ovulation synchronization protocol with the double Ovsynch program (Souza *et al.* 2008) using 100 mg GnRH (gonadorelin diacetate tetrahydrate; Ovacyst, Bayer Animal Health, Whippany, NJ, USA) i.m. 53 ± 3 d post partum followed by 25 mg prostaglandin (PG) $F_{2\alpha}$ (dinoprost tromethamine; Prostamate, Bayer) i.m. 60 ± 3 d post partum. The contents of the pre-ovulatory follicle were aspirated by transvaginal ultrasounography on d 63 ± 3 postpartum (see below for details), immediately before cows received a second GnRH injection 72 h after $PGF_{2\alpha}$. A second Ovsynch protocol was then started 7 d later, and the final GnRH injection was administered approximately 16 h before

timed AI performed at 80 d postpartum. Pregnancy was diagnosed by transrectal ultrasonography 32 d after timed AI.

Blood was collected from the coccygeal vessels into evacuated tubes containing sodium heparin (Vacutainer, Becton Dickson, Franklin Lakes, NJ, USA) on d 7, 21, 35, and 50 post partum. Blood samples were placed on ice prior to centrifugation at 2000 $_{x}$ *g* for 10 min to collect plasma, which was stored at −20°C.

Granulosa Cell Isolation by Ultrasound Guided Transvaginal Follicle Aspiration—The dominant follicle was sampled 63 ± 3 d post partum following a caudal epidural injection of 60 mg of lidocaine hydrochloride 2% (Aspen Veterinary Resources, Greely, CO, USA). The perineum and vulva were cleaned and disinfected with povidone iodine followed by 70% ethanol. Vagina lavage with 100 mL of 0.2% chlorohexidine was followed by two washes with 100 mL sterile 0.9% saline. An oocyte pick-up instrument including a 7.5 MHz convex ultrasound probe (Choice Medical, South Pasadena, FL, USA) was covered in a sanitary sleeve (IMV Technologies, Normandy, France) and introduced into the vagina with sterile lubricant. The ovary was visualized by ultrasound (Aloka SSD-500, Hitachi Healthcare Americas, Twinsburg, OH, USA), and the internal diameter of the dominant follicle was measured based on the average of two measurements at 90° angle of the diameters from the larger cross sectional area of the follicle. An 18 gauge needle attached to a tygon tube connected to a vacuum pump was introduced into the oocyte pick-up instrument and the dominant follicle aspirated into collection medium (Medium 199 with Earle's Salts, 0.5% BSA, 20 mM HEPES, 2 mM sodium pyruvate, 10 IU/mL heparin 100 U/mL penicillin and 100 μg/mL streptomycin; all Fisher Scientific, Hampton NH). The needle was maintained inside the follicle and a total of 10 mL of collection medium was infused through the needle to flush the follicle in 2 mL increments. The volume of aspirate was recorded prior to centrifugation at 300 $_{x}$ *g* for 10 min to separate the follicular fluid from granulosa cells, which were washed twice in sterile PBS. The follicular fluid and granulosa cells were stored at −80°C.

Quantification of LPS, Interleukin-8, Estradiol, Progesterone, Cholesterol and Glucose—Follicular fluid samples were thawed, vortexed for 3 min, and diluted 1:10 in PBS (Gibco 10010–015, pH 7.35). To exclude potential suppression of the assay by endogenous factors, samples were heat-treated at 75°C for 30 min, as described previously (Herath *et al.* 2007). The concentrations of LPS were determined using a Pierce Chromogenic Endotoxin Quant Kit (Thermo Scientific, Waltham, MA, USA) according to the manufacturer's instructions, with minor modifications. Briefly, 50 μL/well standards (from 0.1 to 5 EU/mL LPS), a medium blank, and samples were added to a 96 well plate (Nunclon; Thermo Fisher Scientific, Waltham, MA, USA) on a heating block at 37°C. Then, 50 μL/well ameobcyte lysate reagent was added and the plate incubated for 14 min, prior to addition of 100 μL/well chromogenic substrate reagent for 6 min. The reaction was stopped using 50 μL/well 25% acetic acid, and the optical density at 405 nm was measured using a microplate reader (POLARstar Omega; BMG Labtech, Offenburg, Germany). Concentrations of LPS were determined using linear regression calculated by the microplate reader software. Where samples exceeded the highest standard, samples were further diluted

in PBS and assayed until OD_{405} were within the standard range. The follicular fluid collection medium did not interfere with the assay, and no LPS was detected in three control samples of follicular fluid, obtained from ovaries collected from 2-year old beef heifers with no gross evidence of genital disease or microbial infections, after they were slaughtered and processed as part of the normal work of an abattoir. These control samples were also spiked with a range of concentrations of LPS from 1 to 50 EU/mL, and processed by dilution and heating exactly as for the experimental samples. The control follicular fluid did not contain detectable LPS, and the recovery of spiked LPS was > 90%. The intra- and inter-assay CV was 4.0 and 7.2% respectively and the limit of detection was 0.1 EU/mL.

Follicular fluid IL-8 was measured by bovine specific ELISA as previously described (Cronin *et al*. 2015); using monoclonal mouse anti-ovine IL-8 capture antibody (MCA1660; Bio-Rad, Hercules, CA, USA), recombinant bovine IL-8 protein (RP0023B; Kingfisher Biotech, Saint Paul, USA), polyclonal rabbit anti-sheep IL-8 detection antibody (AHP425; Bio-Rad) and HRP-conjugated goat anti-rabbit (P0448; Dako, Glostrup, Denmark). The intra- and inter-assay CV was 3.2 and 5.4% respectively, and the limit of detection was 62.5 pg/mL.

Follicular fluid glucose was analyzed using a colorimetric method (Randox Daytona Plus, Randox Laboratories Ltd., Crumlin, UK). Glucose concentrations were determined after enzymatic oxidation in the presence of glucose oxidase; the intensity of the final color is directly proportional to the glucose concentration, measured at OD_{505}. The reportable range for glucose on the RX Daytona Plus is 0.2 to 46.5 mM/L.

Follicular fluid total cholesterol concentrations were analyzed with the cholesterol oxidase-enzymatic endpoint method (Randox Daytona Plus). The concentration of cholesterol is determined after enzymatic hydrolysis and oxidation. The reportable range for cholesterol on the RX Daytona Plus is 0.65 to 16 mM/L.

Follicular fluid estradiol and plasma progesterone were quantified using a commercial ELISA according to the manufacturer's instructions (DRG International, Springfield, NJ, USA). The estradiol and progesterone assays were validated using spike-in/recovery performance based on actual and expected recovery of standards supplied with the kits. Recovery of spike-in estradiol was 88.9% to 107.4% of expected estradiol, and recovery of spike-in progesterone was 89% to 101.8% of expected progesterone. The intra-assay CV was 6.5% for estradiol and 7.4% for progesterone.

Isolation, Purification and Sequencing of Granulosa Cell RNA

Granulosa cells were thawed and resuspended in RLT buffer for RNA extraction using the RNeasy Micro kit (Qiagen, Valencia, CA, USA) according to the manufacturer's instructions. Total RNA concentration was determined using a Qubit 2.0 Fluorometer (Thermo Fisher Scientific) and RNA quality was assessed using an Agilent 2100 Bioanalyzer (Agilent Technologies, Santa Clara, CA, USA). Total RNA with a 28S to 18S ratio > 1 and RNA integrity number (RIN) ≥ 7 were used for RNAseq library construction.

To produce RNAseq libraries, 200 ng of total RNA was used to isolate mRNA using NEBNext Poly(A) mRNA magnetic isolation module (New England Biolabs, Ipswich, MA, USA) and RNA library construction with NEBNext Ultra RNA Library Prep Kit for Illumina (New England Biolabs) according to the manufacturer's instructions. Briefly, extracted mRNA was fragmented in NEBNext first strand synthesis buffer by heating at 94°C, followed by first strand cDNA synthesis using reverse transcriptase and random primers. Synthesis of double-stranded cDNA was performed using the 2nd strand master mix provided with the kit. The resulting double-stranded cDNA was end-repaired, dA-tailing and ligated with NEBNext adaptors. Finally, libraries were enriched by 12 cycles of amplification and purified by Meg-Bind RxnPure Plus beads (Omega Biotek, Norcross, GA, USA).

Barcoded libraries were sized on a bioanalyzer, quantitated by QUBIT and qPCR (Kapa Biosystems Wilmington, MA, USA). Eighteen individual libraries were pooled at equal molar concentrations (20 nM), and total of 4 lanes of 2_x 100 bp were run on an Illumina HiSeq3000 (Illumina, San Diego, CA, USA). The RNA library construction and sequencing was performed at the Interdisciplinary Center for Biotechnology Research (ICBR), University of Florida.

Read Mapping, Gene Expression Analysis and Pathway Analysis of Differentially Expressed Genes

Reads acquired from the sequencing platform were cleaned with the Cutadapt program (Martin 2011) to trim off sequencing adaptors, low quality bases, and potential errors introduced during sequencing or library preparation. Reads with a quality Phred-like score < 20 and read length < 40 bases were excluded from RNAseq analysis.

The transcripts of *Bos taurus* (80,896 sequences) retrieved from the NCBI RefSeq database were used as reference sequences for RNAseq analysis. The cleaned reads of each sample were mapped individually to the reference sequences using the bowtie2 mapper (v. 2.2.3) with a '3 mismatches a read' allowance (Langmead & Salzberg 2012). The mapping results were processed with the samtools and scripts developed in house at the University of Florida ICBR to remove potential PCR duplicates and choose uniquely mapped reads for gene expression analysis. Gene expression between the control and treatment group was assessed by counting the number of mapped reads for each transcript (Yao & Yu 2011). Significant up and down regulated genes were selected using the *P*-value and fold-change. Adjusted *P*-values were all above the 0.10 cut-off, as such all data presented for differentially expressed genes are non-adjusted *P* values.

Pathway analysis was performed using Ingenuity Pathway Analysis (Qiagen). Differentially expressed genes with a *P*-value ≤ 0.05 and $\log_2$ FC < −2 or > 2 were used for analysis. Represented canonical pathways with a -log *P*-value > 1.3 were determined with corresponding z-scores to describe predicted activation status. Represented gene networks were determined by assessing the number of differentially expressed genes in a given gene network. Upstream regulators of specific gene networks and upstream regulators of differentially expressed genes were predicted using IPA algorithms. Predicted upstream regulators of differentially expressed genes were assigned an activation z-score to predict the

appropriate upregulation or down regulation of various downstream differentially regulated genes. A z-score ≥ 2 or ≤ −2 was assumed to be a significant prediction of activation or inhibition, respectively. All RNAseq data are reported as $\log_2$ FC.

Statistical Analysis

Disease incidence, parity and fertility were analyzed using the GLIMMIX procedure of SAS v. 9.4 (SAS Institute, Cary, NC) and the model included the fixed effect of group (control vs. metritis). Plasma progesterone concentration was used to determine ovarian cyclicity. Each cow was considered as an individual observation and cyclicity was analyzed as a binary variable at the first plasma sample with progesterone concentration ≥ 1 ng/mL (0 = did not occur; 1 = occurred) and survival analysis was performed using the Gehan-Breslow-Wilcoxon test. Dominant follicle diameter and follicular fluid parameters were analyzed using the GLM procedure of SAS and the model included the fixed effect of disease (metritis). Yields of milk and milk components, concentration of components in milk, and body weight were analyzed using the MIXED procedure of SAS and the models included the fixed effects of group (control vs. metritis), day of measurement, and their interaction. Body weight was used as a covariate to evaluate milk yield. Cow nested within group was considered as a random effect. First order autoregressive covariance structure AR (1) was used as the covariate structure. Principal component analysis plots and heatmaps were generated using online ClustVis tools (Metsalu & Vilo 2015). Values are reported as LSM ± SEM for all parameters except for the RNAseq gene expression analysis. Differences with $P \leq 0.05$ were considered statistically significant.

RESULTS

Health, milk production and follicle parameters in cows with metritis

Of the 45 cows in the study, 17 were diagnosed with metritis within 21 d of parturition, and the remaining 28 cows were considered controls. Lactation number did not differ ($P = 0.94$) between cows with metritis and control cows (2.2 ± 0.3 vs 2.2 ± 0.2). The cows in the two groups had a similar incidence of dystocia (3/17 vs 1/28, $P = 0.11$) and lameness (0/17 vs 3/28). However, cows that had metritis had greater ($P < 0.01$) incidence of ketosis than control cows (70.6% [12/17] vs 21.4% [6/28]). Other diseases including mastitis and displaced abomasum were combined into a single group and were not different between the two groups of cows (25.0% [8/17] vs 47.1% [7/28]). During the first 280 days after parturition, the body weight of cows with metritis was 21.0 ± 6.6 kg lighter ($P < 0.05$) than that of control cows (Supplemental Table 1). In addition, cows diagnosed with metritis produced less ($P < 0.05$) milk (4.6 kg/d), and less ($P < 0.01$) individual components in the milk including fat (0.10 kg/d), true protein (0.10 kg/d), and lactose (0.20 kg/d) than control cows (Supplemental Table 1).

The median days to the return of ovarian cyclic activity was longer ($P = 0.02$) for cows that had metritis than control cows (35 vs 50 days, Supplemental Fig. 1). The subsequent pregnancies as a proportion of inseminations was 28.9% in metritis cows, compared with 39.7% in control cows ($P = 0.43$), although the number of cows examined does not present statistical power to observe differences in pregnancy rates between groups. The diameter of

the aspirated dominant follicle did not differ between groups (Fig. 1A). At the time of follicle aspiration the number of cows at diestrus did not differ between groups (76.5% [13/17] vs 85.7% [24/28]). A total of 34 out of the 45 cows underwent successful follicle aspiration (control n = 19; metritis n = 15) and endometrial cytology confirmed that no cows in the study presented subclinical endometritis at the time of follicle aspiration. Follicular fluid aspirate concentrations of estradiol, IL-8, LPS, glucose and cholesterol did not differ between metritis and control cows (Fig. 1B–F). However, there was a positive association between the concentrations of IL-8 and LPS or glucose ($P < 0.05$), but not cholesterol (Fig. 1G–I).

Differentially expressed genes associated with metritis

RNAseq technology was employed to explore whether metritis had long-term effects on gene expression of granulosa cells. Only clean follicle aspirates with no visible blood contamination were subjected to RNAseq. A total of 7 granulosa cell preparations from cows that had resolved metritis by day 21 were compared with granulosa cell preparations from 9 control cows. The granulosa cell samples yielded 1.5 ± 0.5 μg RNA with RNA integrity number (RIN) > 7.5 (mean 9.0 ± 0.2). Following RNAseq and read processing, a total of 574,407,346 high quality reads were used for analysis (approximately 26 million reads per sample). An average of 34% high quality reads was aligned to the reference genome (Supplemental Table 2). A total of 23,308 Genebank identifiers were identified in at least one sample. The data discussed here have been deposited in NCBI's Gene Expression Omnibus and are accessible through GEO Series accession number GSE128697 (https://www.ncbi.nlm.nih.gov/geo/query/acc.cgi?acc=GSE128697). The highest expressed genes in granulosa cells from both metritis and control cows were *INHBA* (inhibin beta A, 316,390 base mean reads), *SERPINE2* (serpin family E member 2, 270,521 base mean reads), *GSTA3* (glutathione S-transferase alpha 3, 213,755 base mean reads), *LRP8* (LDL receptor related protein 8, 134,090 base mean reads), and *CYP19A1* (cytochrome P450, family 19, subfamily A, polypeptide 1, 116,836 base mean reads).

Unbiased analysis of the RNAseq data for granulosa cells collected from metritis cows yielded 177 genes that had > 2-$\log_2$ fold change (FC), of which 53 genes had > 10-FC, compared with control cows. Of the 177 differentially expressed genes, 144 were upregulated and 33 were down regulated genes, as detailed in Supplemental Table 3, and presented in a volcano plot highlighting their relative $\log_2$ FC (Fig. 2A). Principal component analysis of the 177 differentially expressed genes clustered the metritis cows and control cows into two distinct clusters (Fig. 2B). A heatmap and hierarchical clustering of differentially expressed genes demonstrates the relatedness of samples is shown in Figure 3. The five most upregulated genes in granulosa cells from metritis cows were *ITLN1*, *NCF2*, *CLRN3*, *FSIP2* and *ANKRD17*, and the most downregulated genes in granulosa cells from animals with metritis were *ACSM1*, *NR4A2*, *GHITM*, *CBARP* and *NR1I3* (Table 1).

Selective inspection of the RNAseq data for genes encoding inflammatory cytokines revealed a 3.1 $\log_2$ FC increased ($P = 0.037$) in *IL18* expression in granulosa cells from metritis cows and a tendency ($P = 0.083$) for a 6.7 $\log_2$ FC increase in expression of *CXCL2* and a 2.7 $\log_2$ FC increase ($P = 0.099$) in expression of *IL1A*. Amongst the genes involved

in steroid hormone synthesis, metritis was associated with a 2.3 $\log_2$ FC increase ($P = 0.048$) in expression of *HSD17B2* and a non-significant reduction in the expression of *CYP11A1*, *CYP19A1*, and *STAR* (−0.5, −0.8 and −1.3 $\log_2$ FC, respectively). Analysis of genes involved in cell viability revealed a 2.8 $\log_2$ FC increased ($P = 0.055$) expression of *BCL2L12* in granulosa cells from cows with metritis, and a non-significant increase in expression of *CCNB2*, *CCND1*, and *CASP4* (0.6, 0.6 and 0.5 $\log_2$ FC, respectively). In addition, a −2.1 $\log_2$ FC reduction ($P = 0.053$) of *LHCGR* was observed in cows with metritis. A full list of selected genes is described in Supplemental Table 4.

Annotation and Pathway Analysis of Differentially Expressed Genes

Significantly affected canonical pathways enriched by genes differentially expressed in granulosa cells of cows with metritis are shown in Figure 4. Of the 39 significantly affected canonical pathways, 8 pathways had significant positive z-scores suggesting an upregulation of the pathway due to the distinct pattern of differentially regulated genes. These pathways included Th1 pathway, cholecystokinin/gastrin-mediated signaling, neuro-inflammation signaling, thrombin signaling, actin cytoskeleton signaling, phospholipase C signaling, CXCR4 signaling, and signaling by Rho family GTPases. Of the significantly affected canonical pathways, 18 canonical pathways are involved in immunity or inflammation.

Further analysis revealed 17 gene networks that were impacted in the granulosa cells collected from cows with metritis (Supplemental Table 5). The highest scored gene networks included: 1) developmental disorder, neurological disease, cardiovascular disease; 2) cell-to-cell signaling and interaction, hematological system development and function, immune cell trafficking; 3) cell signaling, molecular transport, nucleic acid metabolism; 4) cell cycle, cellular assembly and organization, DNA replication, recombination, and repair; 5) cancer, cellular development, organismal injury and abnormalities; and 6) cellular function and maintenance, cellular growth and proliferation, amino acid metabolism (Table 2). The involvement of specific differentially regulated genes in the cell-to-cell signaling and interaction, hematological system development and function, immune cell trafficking is shown in Fig. 5A; cell signaling, molecular transport, nucleic acid metabolism network is shown in Fig. 5B; and developmental disorder, neurological disease, cardiovascular disease is shown in Fig. 5C.

Twelve molecules were predicted as significant upstream regulators of differentially expressed genes in metritis animals (Table 3). The predicted upstream regulators of affected gene networks included IL-12 and IL-21, which are involved in stimulation of lymphocyte and cytolysis gene networks, respectively (Fig. 6A–B), and NF-κB and *E. coli* LPS, which are involved in innate immunity (Fig. 6C–D).

DISCUSSION

Here we examined whether metritis was associated with changes in the transcriptome of granulosa cells from dominant follicles of dairy cows 6 weeks after the resolution of disease. The granulosa cells from metritis cows had 177 differentially expressed genes compared with control cows, and these were associated with pathways such as immune function, cell-cell communication, cell cycle and cellular metabolism. Interestingly, the predicted upstream

gene regulators included NFκB, IL-21 and LPS, which are all associated with immune responses. Taken together, these data provide evidence that metritis leaves a persistent mark on the granulosa cell transcriptome, which could negatively impact ovarian function, oocyte health, and fertility.

We evaluated granulosa cells from dominant follicles 63 days post partum, which means the follicles were in their early stages of development during active disease. The RNAseq analysis of cells aspirated from dominant follicles revealed *INHBA* and *CYP19A1* were among the 5 highest expressed genes in samples, confirming that the majority of cells sequenced were granulosa cells of large follicles (Hatzirodos *et al.* 2014, Hatzirodos *et al.* 2017). Among the differentially expressed granulosa cell genes, 144 were upregulated and 33 genes were down regulated. The highest upregulated gene in metritis cows was intelectin 1 (*ITLN1*), a carbohydrate binding protein which recognizes bacterial glycans (Wesener *et al.* 2015). The increased *ITLN1* expression may reflect an effect of metritis on the transcriptome that persisted after resolution of disease or from persistent exposure to pathogen-associated molecular patterns. It was notable that LPS was detectable in follicular fluid of all cows in concentrations that did not differ between groups, although they were lower than in follicular fluid from cows with active endometritis (Herath *et al.* 2007). Because these cows were 63 ± 3 d postpartum when follicles were aspirated, at least 6 weeks after the resolution of the disease, it is not surprising that concentrations of LPS in the follicular fluid did not differ between groups. We suggest that differences that might have occurred early in lactation during active disease (Herath *et al.* 2007) likely equalized over time and the values detected at 63 days postpartum likely reflected the background exposure from LPS of other origins such as rumen or miscellaneous bacterial infections. Nevertheless, granulosa cells increase secretion of IL-8 in response to LPS (Bromfield & Sheldon 2011), and in the present study there was a positive association between IL-8 and LPS in follicular fluid. The responsiveness of cells to LPS is also glucose dependent (Turner *et al.* 2016), and we also noted a positive association between IL-8 and glucose in follicular fluid. Interestingly, predictions for upstream regulators of differentially expressed genes in the metritis cows included LPS and NFκB. Granulosa cells respond to LPS via the innate immune receptor Toll-like receptor 4 (Herath *et al.* 2007, Bromfield & Sheldon 2011), and NFκB is central to innate immune responses (Moresco *et al.* 2011).

The analysis of 177 differentially regulated genes described 39 significantly affected canonical pathways, including 18 pathways associated with immune response, including Th1 pathway, Th1 and Th2 activation, natural killer cell signaling, and cross talk between dendritic cells. Th1 and Th2 cells are involved in the adaptive immune response to bacteria and parasites, respectively, as well as in the transition from innate to cell mediated immunity (Romagnani 1999). Knowledge about the adaptive immune response during metritis is less advanced than for innate immunity, which initially dominates the endometrial response to infection (Herath *et al.* 2009, Sheldon & Roberts 2010). Prediction of downstream pathways regulated by differentially expressed genes also included stimulation of lymphocytes, further implicating a role of the adaptive immune response in cows with metritis after the resolution of disease. Although the ovarian follicle is normally deplete of hematopoietic immune cells prior to ovulation (Bromfield & Sheldon 2013), we identified canonical pathways and gene networks associated with immune cell trafficking. While not investigated here, it may be

prudent to further explore whether immune cells traffic into follicles of cows with metritis in future studies.

When evaluating other genes involved in immunity, most presented a non-significant numerical increase in expression in metritis cows, including ankyrin repeat domain-containing protein 17 (*ANKRD17*), chemokine ligand 2 (*CXCL2*) and *IL18*. The gene *ANKRD17* was upregulated 4.8-$\log_2$ fold in granulosa cells of metritis cows, and is associated with antibacterial innate immune activation by the nucleotide-binding domain and leucine-rich repeat (NLR) receptors, NOD1 and NOD2 (Menning & Kufer 2013). As a chemokine, *CXCL2* is a neutrophil chemoattractant secreted in response to LPS (Wolpe & Cerami 1989) and may increase the recruitment of innate immune cells to the ovary of cows with metritis. The cytokine IL-18 is involved in the initiation of cell mediated immunity and increases interferon production by natural killer cells (Netea *et al*. 2015). Expression of neutrophil cytosolic factor 2 (*NCF2*) was increased 7.9-$\log_2$ fold in metritis cows. Neutrophil cytosolic factor 2 is a cofactor of NADPH oxidase, important in immune cell function and phagocytosis. Increased NCF2 activity likely also increases potential for reactive oxygen accumulation which reduces oocyte developmental competence (Tamura *et al*. 2008, Lai *et al*. 2018). Increased granulosa cell *NCF2* expression has been implicated in poorer follicle quality of patients with polycystic ovarian syndrome (Kaur *et al*. 2012).

Ovulation has been described as an inflammatory event (Espey 1980, Spanel-Borowski 2011). It is possible that the immunological events described here by RNAseq may be a reflection in the differential capacity of cows with metritis to ovulate in a timely manner in response to estrous synchronization. Cows with uterine inflammation have slower growing follicles and are less likely to ovulate (Suzuki *et al*. 2001, Sheldon *et al*. 2002, Williams *et al*. 2007, Williams *et al*. 2008). In the present study, expression of the LH receptor (*LHCGR*) was −2.1 $\log_2$-fold lower in granulosa cells of metritis cows than control cows; a decrease in expression which may alter the capacity of the dominant follicle to respond to ovulatory LH. While pathway analysis did not highlight endocrine function, we evaluated expression of genes involved in steroidogenesis because of their importance in granulosa cell function (Adashi *et al*. 1985). In vitro, granulosa cells decrease estradiol secretion when exposed to LPS as a result of reduced *CYP19A1* expression (Herath *et al*. 2007). In the present study, granulosa cells from metritis cows had non-significant reductions in expression of genes involved in steroidogenesis, including *CYP11A1, CYP19A1, HSD3B1* and *STAR*, but follicular fluid estradiol concentrations did not differ significantly from control cows. It may be that granulosa cell endocrine function in cows is no longer effected after the resolution of disease. This is in contrast to previous investigations using cows with resolved subclinical endometritis that had reduced estradiol in 8 to 10 mm follicles, follicles considerably smaller than those assessed here (Green *et al*. 2011).

Analysis of gene networks enriched amongst differentially expressed genes in metritis cows revealed that cell-cell signaling, molecular transport, cell cycle, DNA repair and cellular metabolism were down regulated. Granulosa cell function is critical in providing oocyte with required nutrition in the form of carbohydrates and lipids, in addition to maintaining oocyte meiotic arrest and the induction of oocyte maturation (Sugiura *et al*. 2007, Su *et al*. 2008, Bromfield & Piersanti 2019). Furthermore, communication between granulosa cells and the

oocyte is facilitated by soluble secreted factors and direct cell-cell communication via transzonal projections (Matzuk *et al.* 2002, Albertini & Barrett 2003). Perturbing granulosa cell metabolism or communication could reduce oocyte quality and the capacity to develop through the blastocyst stage. Alterations to granulosa cell function have been associated with reduced fertility in ageing women (Tatone & Amicarelli 2013), while it has been suggested that other human pathologies have granulosa function as a component of infertility (Toya *et al.* 2000, Gioacchini *et al.* 2018). Collectively, we suggest that the alterations in granulosa cell transcriptome may contribute to reduced fertility typically observed in cows previously diagnosed with metritis.

In conclusion, our data provide evidence that postpartum metritis has an enduring effect on the granulosa cell transcriptome of dominant follicles 6 weeks after resolution of the disease. Collectively, we propose that these disease-dependent changes in the granulosa cell transcriptome could impair the follicle microenvironment and oocyte health. Understanding the mechanisms by which disease impacts long-term granulosa cell transcriptome is an important step in attempting to minimize the negative consequences of uterine disease on fertility.

Supplementary Material

Refer to Web version on PubMed Central for supplementary material.

ACKNOWLEDGEMENTS

The authors would like to thank Todd Pritchard, Miguel Torrado and the staff at the University of Florida Dairy Research Unit. In addition, we would like to extend our gratitude to the University of Florida ICBR staff, Dr Fahong Yu and Yanping Zhang, for assistance with RNAseq and bioinformatics. We would also like to thank Jason Rizo, Paula Molinari and Amanda Teixeira for their contributions during the study.

FUNDING

Research reported in this publication was supported by the Eunice Kennedy Shriver National Institute of Child Health & Human Development of the National Institutes of Health under Award Number R01HD084316. The content is solely the responsibility of the authors and does not necessarily represent the official views of the National Institutes of Health.

REFERENCES

Adashi EY, Resnick CE, D'Ercole AJ, Svoboda ME & Van Wyk JJ 1985 Insulin-like growth factors as intraovarian regulators of granulosa cell growth and function. Endocrine Reviews 6 400–420. [PubMed: 2992919]

Albertini DF & Barrett SL 2003 Oocyte-somatic cell communication. Reproduction Supplement 61 49–54.

Amos MR, Healey GD, Goldstone RJ, Mahan SM, Duvel A, Schuberth HJ, Sandra O, Zieger P, Dieuzy-Labaye I, Smith DG & Sheldon IM 2014 Differential endometrial cell sensitivity to a cholesterol-dependent cytolysin links Trueperella pyogenes to uterine disease in cattle. Biology of Reproduction 90 54. [PubMed: 24478394]

Bicalho ML, Machado VS, Oikonomou G, Gilbert RO & Bicalho RC 2012 Association between virulence factors of Escherichia coli, Fusobacterium necrophorum, and Arcanobacterium pyogenes and uterine diseases of dairy cows. Veterinary Microbiology 157 125–131. [PubMed: 22186615]

Britt JH, Cushman RA, Dechow CD, Dobson H, Humblot P, Hutjens MF, Jones GA, Ruegg PS, Sheldon IM & Stevenson JS 2018 Invited review: Learning from the future-A vision for dairy farms and cows in 2067. Journal of Dairy Science 101 3722–3741. [PubMed: 29501340]

Bromfield JJ & Piersanti RL 2019 Mammalian Oogenesis: The Fragile Foundation of the Next Generation In The Ovary, pp. 157–164.

Bromfield JJ & Sheldon IM 2011 Lipopolysaccharide initiates inflammation in bovine granulosa cells via the TLR4 pathway and perturbs oocyte meiotic progression in vitro. Endocrinology 152 5029–5040. [PubMed: 21990308]

Bromfield JJ & Sheldon IM 2013 Lipopolysaccharide reduces the primordial follicle pool in the bovine ovarian cortex ex vivo and in the murine ovary in vivo. Biology of Reproduction 88 98. [PubMed: 23515670]

Bromfield JJ, Watt MM & Iacovides SM 2018 Characterisation of peripheral blood mononuclear cell populations in periparturient dairy cows that develop metritis. Veterinary Immunology and Immunopathology 200 69–75. [PubMed: 29776614]

Canipari R 2000 Oocyte--granulosa cell interactions. Human Reproduction Update 6 279–289. [PubMed: 10874573]

Cronin JG, Hodges R, Pedersen S & Sheldon IM 2015 Enzyme linked immunosorbent assay for quantification of bovine interleukin-8 to study infection and immunity in the female genital tract. American Journal of Reproductive Immunology 73 372–382. [PubMed: 25427847]

Espey LL 1980 Ovulation as an inflammatory reaction--a hypothesis. Biology of Reproduction 22 73–106. [PubMed: 6991013]

Gioacchini G, Notarstefano V, Sereni E, Zaca C, Coticchio G, Giorgini E, Vaccari L, Carnevali O & Borini A 2018 Does the molecular and metabolic profile of human granulosa cells correlate with oocyte fate? New insights by Fourier transform infrared microspectroscopy analysis. Molecular Human Reproduction 24 521–532. [PubMed: 30124927]

Green MP, Ledgard AM, Beaumont SE, Berg MC, McNatty KP, Peterson AJ & Back PJ 2011 Long-term alteration of follicular steroid concentrations in relation to subclinical endometritis in postpartum dairy cows. Journal of Animal Science 89 3551–3560. [PubMed: 21666004]

Hatzirodos N, Glister C, Hummitzsch K, Irving-Rodgers HF, Knight PG & Rodgers RJ 2017 Transcriptomal profiling of bovine ovarian granulosa and theca interna cells in primary culture in comparison with their in vivo counterparts. PLoS One 12 e0173391. [PubMed: 28282394]

Hatzirodos N, Irving-Rodgers HF, Hummitzsch K, Harland ML, Morris SE & Rodgers RJ 2014 Transcriptome profiling of granulosa cells of bovine ovarian follicles during growth from small to large antral sizes. BMC Genomics 15 24. [PubMed: 24422759]

Herath S, Lilly ST, Santos NR, Gilbert RO, Goetze L, Bryant CE, White JO, Cronin J & Sheldon IM 2009 Expression of genes associated with immunity in the endometrium of cattle with disparate postpartum uterine disease and fertility. Reproductive Biology and Endocrinology 7 55. [PubMed: 19476661]

Herath S, Williams EJ, Lilly ST, Gilbert RO, Dobson H, Bryant CE & Sheldon IM 2007 Ovarian follicular cells have innate immune capabilities that modulate their endocrine function. Reproduction 134 683–693. [PubMed: 17965259]

Huzzey JM, Veira DM, Weary DM & von Keyserlingk MA 2007 Prepartum behavior and dry matter intake identify dairy cows at risk for metritis. Journal of Dairy Science 90 3220–3233. [PubMed: 17582105]

Jeon SJ, Cunha F, Ma X, Martinez N, Vieira-Neto A, Daetz R, Bicalho RC, Lima S, Santos JE, Jeong KC & Galvao KN 2016 Uterine Microbiota and Immune Parameters Associated with Fever in Dairy Cows with Metritis. PLoS One 11 e0165740. [PubMed: 27802303]

Kaur S, Archer KJ, Devi MG, Kriplani A, Strauss JF 3rd & Singh R 2012 Differential gene expression in granulosa cells from polycystic ovary syndrome patients with and without insulin resistance: identification of susceptibility gene sets through network analysis. Journal of Clinical Endocrinology and Metabolism 97 E2016–2021. [PubMed: 22904171]

Lai Q, Xiang W, Li Q, Zhang H, Li Y, Zhu G, Xiong C & Jin L 2018 Oxidative stress in granulosa cells contributes to poor oocyte quality and IVF-ET outcomes in women with polycystic ovary syndrome. Frontiers in Medicine 12 518–524.

Langmead B & Salzberg SL 2012 Fast gapped-read alignment with Bowtie 2. Nature Methods 9 357–359. [PubMed: 22388286]

LeBlanc SJ, Osawa T & Dubuc J 2011 Reproductive tract defense and disease in postpartum dairy cows. Theriogenology 76 1610–1618. [PubMed: 21890187]

Martin M 2011 Cutadapt Removes Adapter Sequences From High-Throughput Sequencing Reads. EMBnet.journal 17 10–12.

Matzuk MM, Burns KH, Viveiros MM & Eppig JJ 2002 Intercellular communication in the mammalian ovary: oocytes carry the conversation. Science 296 2178–2180. [PubMed: 12077402]

Menning M & Kufer TA 2013 A role for the Ankyrin repeat containing protein Ankrd17 in Nod1- and Nod2-mediated inflammatory responses. FEBS Letters 587 2137–2142. [PubMed: 23711367]

Metsalu T & Vilo J 2015 ClustVis: a web tool for visualizing clustering of multivariate data using Principal Component Analysis and heatmap. Nucleic Acids Research 43 W566–570. [PubMed: 25969447]

Moresco EM, LaVine D & Beutler B 2011 Toll-like receptors. Current Biology 21 R488–493. [PubMed: 21741580]

Netea MG, van de Veerdonk FL, van der Meer JW, Dinarello CA & Joosten LA 2015 Inflammasome-independent regulation of IL-1-family cytokines. Annual Review of Immunology 33 49–77.

Price JC, Bromfield JJ & Sheldon IM 2013 Pathogen-associated molecular patterns initiate inflammation and perturb the endocrine function of bovine granulosa cells from ovarian dominant follicles via TLR2 and TLR4 pathways. Endocrinology 154 3377–3386. [PubMed: 23825132]

Ribeiro ES, Gomes G, Greco LF, Cerri RLA, Vieira-Neto A, Monteiro PLJ Jr., Lima FS, Bisinotto RS, Thatcher WW & Santos JEP 2016 Carryover effect of postpartum inflammatory diseases on developmental biology and fertility in lactating dairy cows. Journal of Dairy Science 99 2201–2220. [PubMed: 26723113]

Romagnani S 1999 Th1/Th2 cells. Inflammatory Bowel Diseases 5 285–294. [PubMed: 10579123]

Santos TM & Bicalho RC 2012 Diversity and succession of bacterial communities in the uterine fluid of postpartum metritic, endometritic and healthy dairy cows. PLoS One 7 e53048. [PubMed: 23300859]

Sheldon IM, Cronin J, Goetze L, Donofrio G & Schuberth HJ 2009 Defining postpartum uterine disease and the mechanisms of infection and immunity in the female reproductive tract in cattle. Biology of Reproduction 81 1025–1032. [PubMed: 19439727]

Sheldon IM, Lewis GS, LeBlanc S & Gilbert RO 2006 Defining postpartum uterine disease in cattle. Theriogenology 65 1516–1530. [PubMed: 16226305]

Sheldon IM, Noakes DE, Rycroft AN, Pfeiffer DU & Dobson H 2002 Influence of uterine bacterial contamination after parturition on ovarian dominant follicle selection and follicle growth and function in cattle. Reproduction 123 837–845. [PubMed: 12052238]

Sheldon IM, Price JC, Turner ML, Bromfield JJ & Cronin J 2014 Uterine infection and immunity in cattle In Reproduction in Domestic Ruminants VIII, pp. 415–430.

Sheldon IM & Roberts MH 2010 Toll-like receptor 4 mediates the response of epithelial and stromal cells to lipopolysaccharide in the endometrium. PLoS One 5 e12906. [PubMed: 20877575]

Sheldon IM, Rycroft AN, Dogan B, Craven M, Bromfield JJ, Chandler A, Roberts MH, Price SB, Gilbert RO & Simpson KW 2010 Specific strains of Escherichia coli are pathogenic for the endometrium of cattle and cause pelvic inflammatory disease in cattle and mice. PLoS One 5 e9192. [PubMed: 20169203]

Soto P, Natzke RP & Hansen PJ 2003 Identification of possible mediators of embryonic mortality caused by mastitis: actions of lipopolysaccharide, prostaglandin F2alpha, and the nitric oxide generator, sodium nitroprusside dihydrate, on oocyte maturation and embryonic development in cattle. American Journal of Reproductive Immunology 50 263–272. [PubMed: 14629032]

Souza AH, Ayres H, Ferreira RM & Wiltbank MC 2008 A new presynchronization system (Double-Ovsynch) increases fertility at first postpartum timed AI in lactating dairy cows. Theriogenology 70 208–215. [PubMed: 18468675]

Spanel-Borowski K 2011 Ovulation as danger signaling event of innate immunity. Molecular and Cellular Endocrinology 333 1–7. [PubMed: 21163330]

Su YQ, Sugiura K, Wigglesworth K, O'Brien MJ, Affourtit JP, Pangas SA, Matzuk MM & Eppig JJ 2008 Oocyte regulation of metabolic cooperativity between mouse cumulus cells and oocytes: BMP15 and GDF9 control cholesterol biosynthesis in cumulus cells. Development 135 111–121. [PubMed: 18045843]

Sugiura K, Su Y-Q, Diaz FJ, Pangas SA, Sharma S, Wigglesworth K, O'Brien MJ, Matzuk MM, Shimasaki S & Eppig JJ 2007 Oocyte-derived BMP15 and FGFs cooperate to promote glycolysis in cumulus cells. Development 134 2593–2603. [PubMed: 17553902]

Suzuki C, Yoshioka K, Iwamura S & Hirose H 2001 Endotoxin induces delayed ovulation following endocrine aberration during the proestrous phase in Holstein heifers. Domestic Animal Endocrinology 20 267–278. [PubMed: 11518620]

Tamura H, Takasaki A, Miwa I, Taniguchi K, Maekawa R, Asada H, Taketani T, Matsuoka A, Yamagata Y, Shimamura K, Morioka H, Ishikawa H, Reiter RJ & Sugino N 2008 Oxidative stress impairs oocyte quality and melatonin protects oocytes from free radical damage and improves fertilization rate. Journal of Pineal Research 44 280–287. [PubMed: 18339123]

Tatone C & Amicarelli F 2013 The aging ovary--the poor granulosa cells. Fertility and Sterility 99 12–17. [PubMed: 23273984]

Toya M, Saito H, Ohta N, Saito T, Kaneko T & Hiroi M 2000 Moderate and severe endometriosis is associated with alterations in the cell cycle of granulosa cells in patients undergoing in vitro fertilization and embryo transfer. Fertil Steril 73 344–350. [PubMed: 10685541]

Turner ML, Cronin JG, Healey GD & Sheldon IM 2014 Epithelial and stromal cells of bovine endometrium have roles in innate immunity and initiate inflammatory responses to bacterial lipopeptides in vitro via Toll-like receptors TLR2, TLR1, and TLR6. Endocrinology 155 1453–1465. [PubMed: 24437488]

Turner ML, Cronin JG, Noleto PG & Sheldon IM 2016 Glucose Availability and AMP-Activated Protein Kinase Link Energy Metabolism and Innate Immunity in the Bovine Endometrium. PLoS One 11 e0151416. [PubMed: 26974839]

Wesener DA, Wangkanont K, McBride R, Song X, Kraft MB, Hodges HL, Zarling LC, Splain RA, Smith DF, Cummings RD, Paulson JC, Forest KT & Kiessling LL 2015 Recognition of microbial glycans by human intelectin-1. Nature Structural & Molecular Biology 22 603–610.

Williams EJ, Fischer DP, Noakes DE, England GC, Rycroft A, Dobson H & Sheldon IM 2007 The relationship between uterine pathogen growth density and ovarian function in the postpartum dairy cow. Theriogenology 68 549–559. [PubMed: 17574659]

Williams EJ, Fischer DP, Pfeiffer DU, England GC, Noakes DE, Dobson H & Sheldon IM 2005 Clinical evaluation of postpartum vaginal mucus reflects uterine bacterial infection and the immune response in cattle. Theriogenology 63 102–117. [PubMed: 15589277]

Williams EJ, Sibley K, Miller AN, Lane EA, Fishwick J, Nash DM, Herath S, England GC, Dobson H & Sheldon IM 2008 The effect of Escherichia coli lipopolysaccharide and tumour necrosis factor alpha on ovarian function. American Journal of Reproductive Immunology 60 462–473. [PubMed: 19238751]

Wolpe SD & Cerami A 1989 Macrophage inflammatory proteins 1 and 2: members of a novel superfamily of cytokines. FASEB Journal 3 2565–2573. [PubMed: 2687068]

Yao JQ & Yu F 2011 DEB: A web interface for RNA-seq digital gene expression analysis. Bioinformation 7 44–45. [PubMed: 21904439]

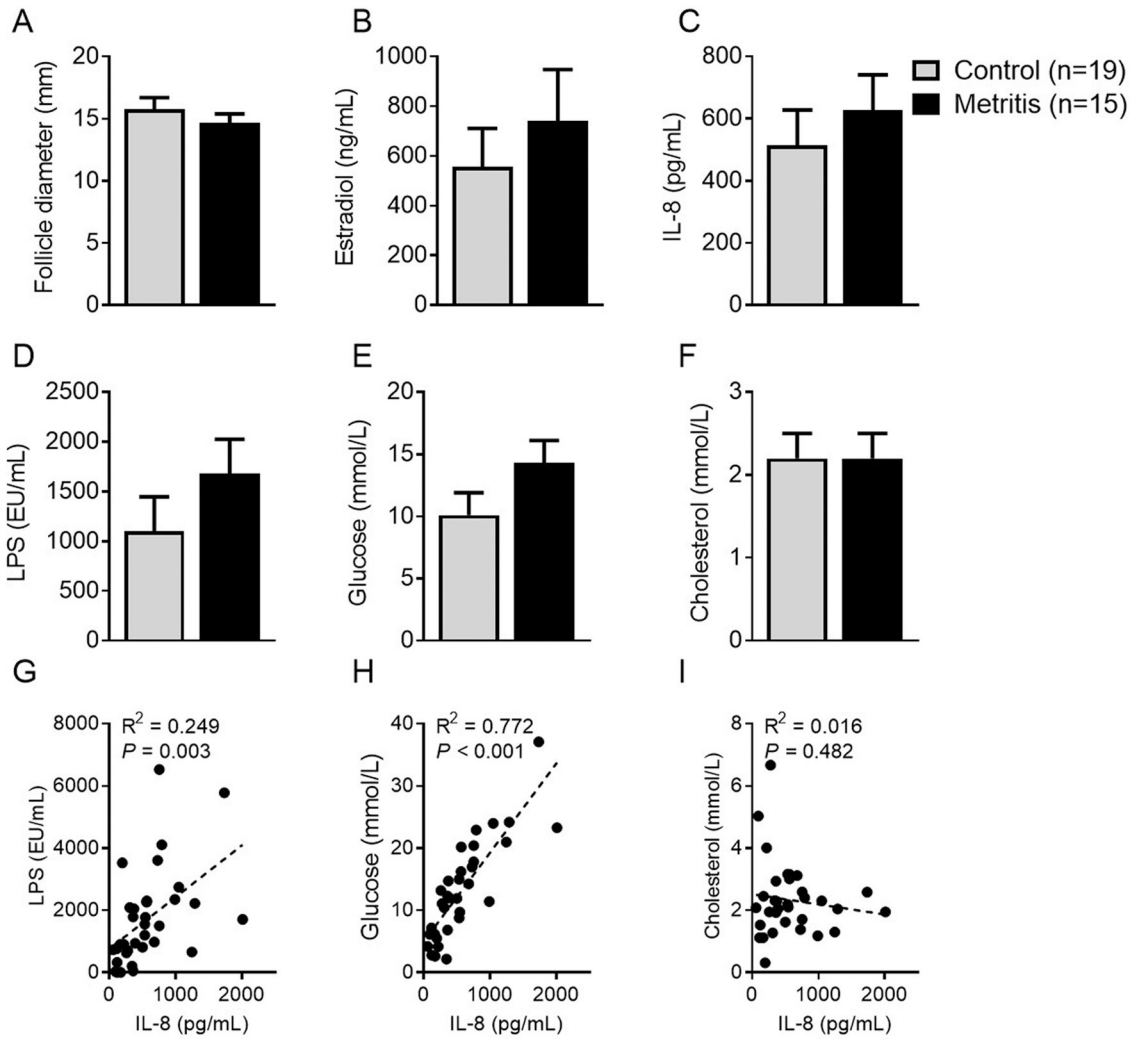

Figure 1. Follicle evaluation 63 days post partum.

Follicular fluid was aspirated on day 63 post partum from control cows (grey bar, n=19) and cows that had metritis during the first 21 days post partum (black bars, n=15). The diameter of each dominant follicle was measured (A). Follicular fluid was evaluated for estradiol (B), IL-8 (C), LPS (D), glucose (E), and cholesterol concentrations (F). Data are presented as LSM + SEM and analyzed using the generalized linear mixed model. Associations between the follicular fluid concentrations of IL-8 and LPS (G), glucose (H), or cholesterol (I) are described.

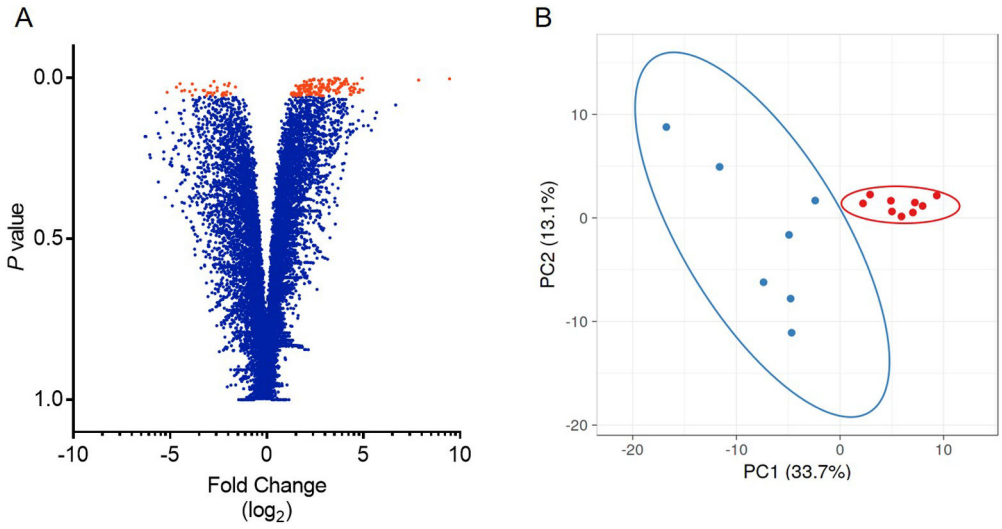

Figure 2. Differentially expressed genes in granulosa cells of cows with metritis.

A volcano plot (A) represents each gene detected using RNAseq as an individual dot. Genes that were differentially regulated in granulosa cells of metritis cows are shown in orange ($P \leq 0.05$), and non-significantly affected genes are shown in blue. Expression of genes is based on the $\log_2$ fold change (x-axis) plotted against the *P* value for each gene. (B) Plot for principal component analysis of RNAseq data from granulosa cells of cows that had metritis (blue) or control cows (red).

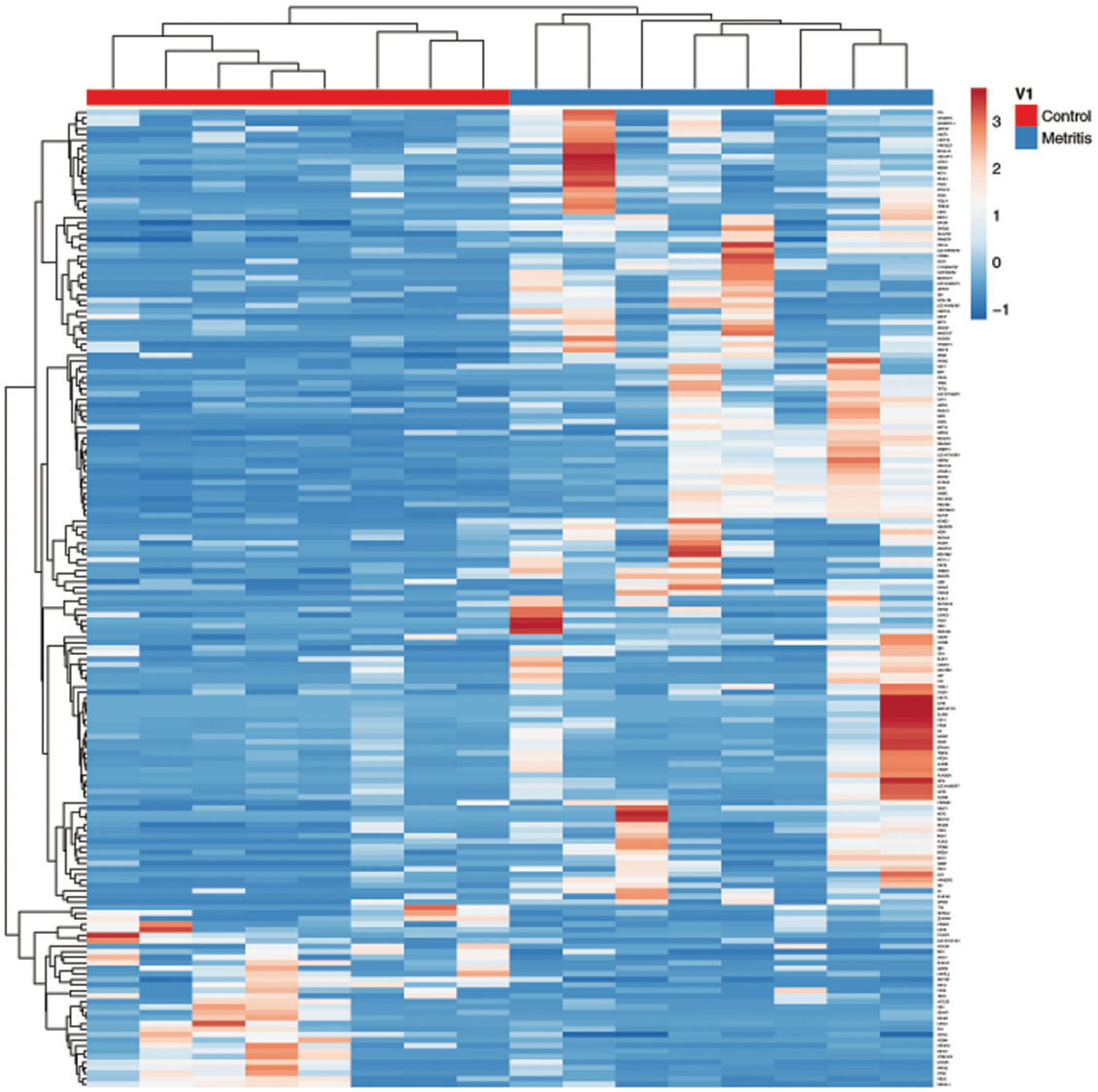

Figure 3. Heatmap of differentially expressed granulosa cell genes in metritis cows.

A heatmap and hierarchical clustering of differentially expressed genes in metritis cows (blue) and control cows (red). Each differentially expressed gene is represented by a single row, and each cow is represented by a single column. Both rows and columns are clustered using correlation distance and average linkage.

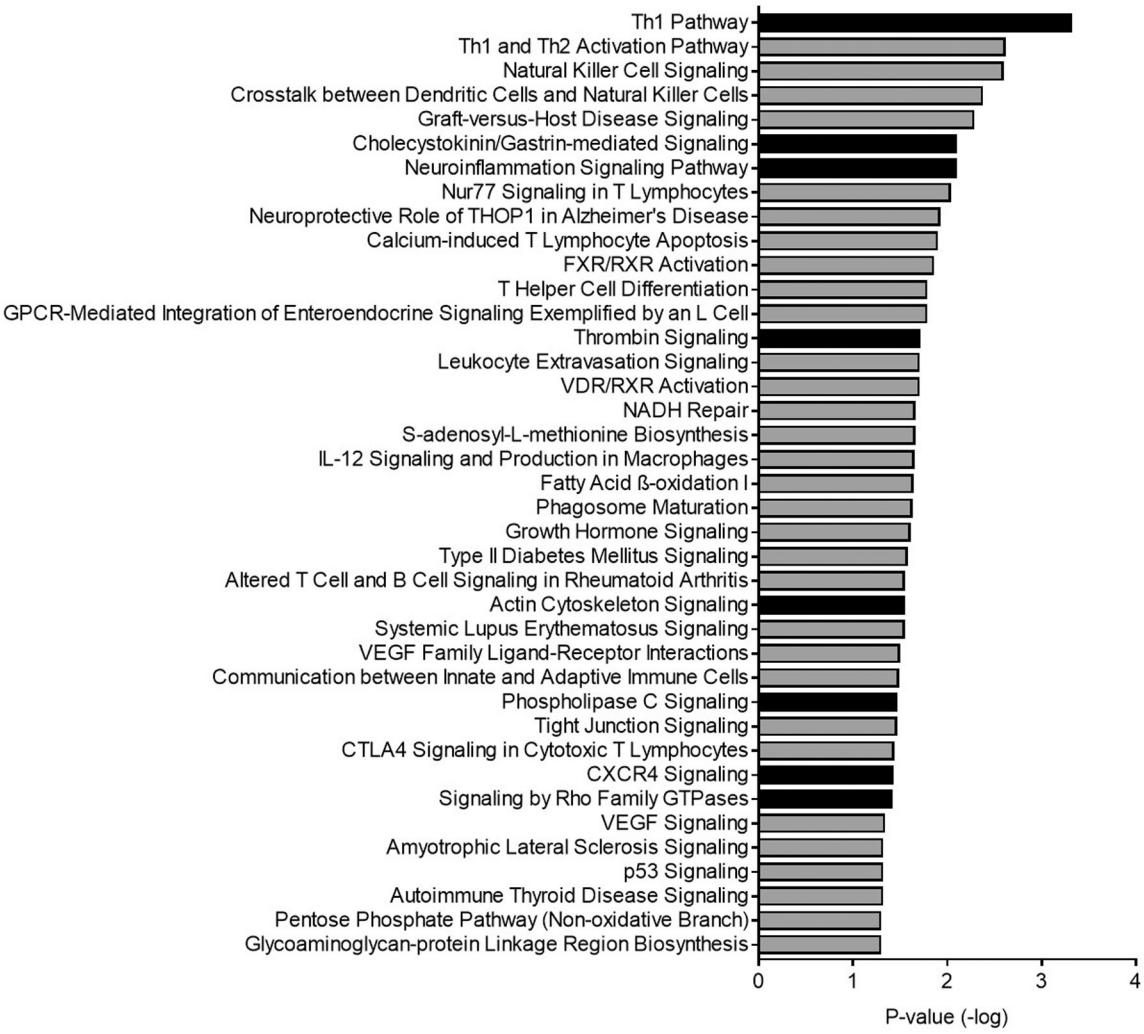

Figure 4. Canonical pathways derived from differentially expressed genes in granulosa cells of cows with metritis.

Depiction of affected canonical pathways identified based on differentially expressed genes in granulosa cells of cows with metritis compared with cells from control cows, with a -log *P* value > 1.3. Solid bars represent canonical pathways with a positive z-score, grey bars represent canonical pathways with no calculable z-score.

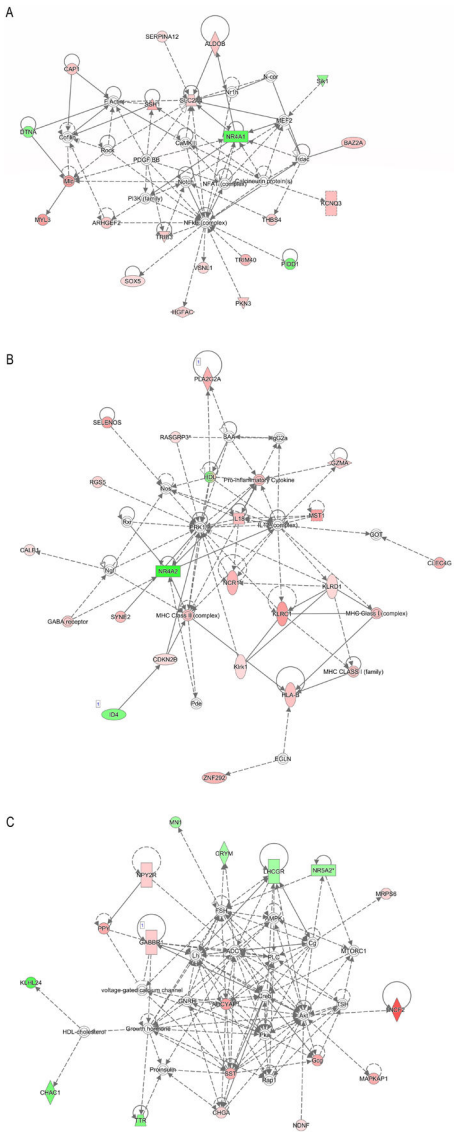

Figure 5. Differentially regulated gene networks in granulosa cells of cows with metritis.

Affected gene networks based on differentially regulated genes of granulosa cells from cows with metritis. (A) cell-to-cell signaling and interaction, hematological system development and function, immune cell trafficking; (B) cell signaling, molecular transport, nucleic acid metabolism; and (C) developmental disorder, neurological disease, cardiovascular disease. Symbols in red are upregulated, and symbols in green are downregulated in granulosa cells of metritis cows.

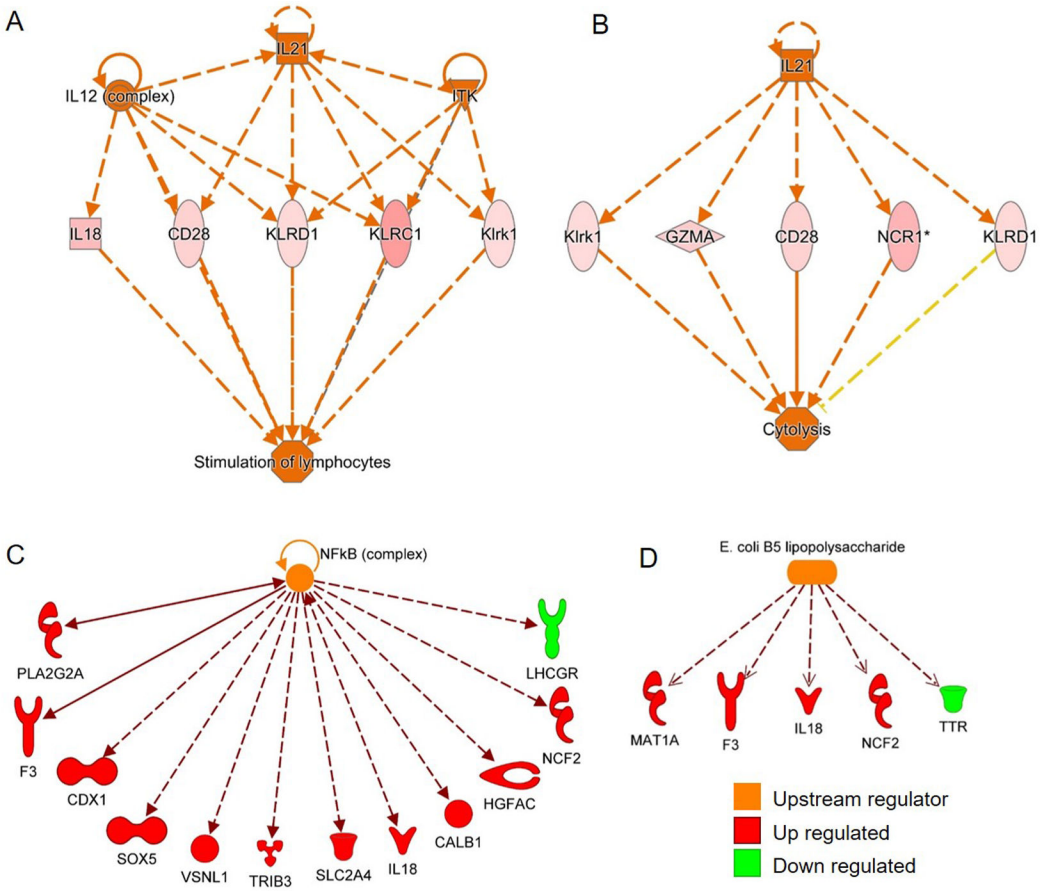

Figure 6. Predicted upstream regulators in granulosa cells of cows with metritis.

The Predicted upstream regulators of affected gene networks included IL-12 (A) and IL-21 (B), which are involved in stimulation of lymphocyte and cytolysis gene networks, respectively. NF-κB (C) and *E. coli* LPS (D) are predicted upstream regulators of differentially expressed genes. Symbols in red are upregulated, and symbols in green are downregulated in granulosa cells of metritis cows. Symbols in orange are predicted upstream regulators of function.

Table 1.

Greatest differentially expressed genes in granulosa cells of cows with metritis.

Gene	Gene name	Control[1]	Metritis[1]	Log_2 FC	*P* value
ITLN1	Intelectin 1	0.3	193.0	9.5	0.002
NCF2	Neutrophil Cytosolic Factor 2	0.1	22.7	7.9	0.006
CLRN3	Clarin 3	0.4	12.5	5.0	0.038
FSIP2	Fibrous Sheath Interacting Protein 2	0.3	8.4	4.9	0.0001
ANKRD17	Ankyrin Repeat Domain 17	0.1	2.7	4.8	0.035
ACSM1	Acyl-CoA Synthetase Medium Chain Family Member 1	4.7	0.1	−5.1	0.044
NR4A2	Nuclear Receptor Subfamily 4 Group A Member 2	5.8	0.2	−4.7	0.028
GHITM	Growth Hormone Inducible Transmembrane Protein	3.0	0.1	−4.5	0.018
CBARP	CACN Subunit Beta Associated Regulatory Protein	2.4	0.1	−4.4	0.040
NR1I3	Nuclear Receptor Subfamily 1 Group I Member 3	2.3	0.1	−4.3	0.038

[1]Base mean values determined by RNAseq read number. FC, fold change.

Table 2

Gene networks enriched amongst genes differentially expressed in granulosa cells from cows with metritis.

Gene network[1]	Network score[2]	Genes differentially expressed[3]	
		Upregulated	Downregulated
Developmental Disorder, Neurological Disease, Cardiovascular Disease	36	*ALDOB, ARHGEF2, BAZ2A, CAP1, HGFAC, KCNQ3, MYL3, PKN3, SERPINA12, SLC2A4, SOX5, SSH1, THBS4, TRIB3, TRIM40, VSNL1*	*DTNA, NR4A1, PIDD1, SIK1*
Cell-To-Cell Signaling and Interaction, Hematological System Development and Function, Immune Cell Trafficking	34	*CALB1, CDKN2B, CLEC4G, GZMA, HLAB, IL18, KLRC1, KLRD1, KLRK1, MST1, NCR1, PLA2G2A, RASGRP3, RGS5, SELENOS, SYNE2, ZNF292*	*ID4, NR4A2*
Cell Signaling, Molecular Transport, Nucleic Acid Metabolism	32	*ADCYAP1, CHGA, GABBR1, GCG, MAPKAP1, MRPS6, NCF2, NDNF, NPY2R, PPY, SST*	*CHAC1, CRYM, KLHL24, LHCGR, MN1, NR5A2, TTR*
Cell Cycle, Cellular Assembly and Organization, DNA Replication, Recombination, and Repair	25	*A4GNT, ARPP19, CCDC63, CLRN3, FAM131A, FAM207A, FANCE, GPR25, HOXC11, PAN3, RAB5C, SLC27A6, TKTL2, VGLL4,*	*HELQ*
Cancer, Cellular Development, Organismal Injury and Abnormalities	23	*C20orf196, CHP2, CRCT1, EIF5A2, FGF14, PCTP, POC5, PRICKLE1, SIX4, SMG8, SPATC1L*	*ACADM, ACSM1, STX17*
Cellular Function and Maintenance, Cellular Growth and Proliferation, Amino Acid Metabolism	21	*ANKRD17, ATOH1, BTN1A1, CD28, CDX1, CNIH4, F3, FGFR3, HSD17B2, MAT1A, PCDH7, VCL*	*PDLIM3*

[1] Enriched gene networks determined by Ingenuity Pathway Analysis using significantly differentially expressed genes only.

[2] Network score is derived from a *P*-value and indicates the likelihood of the genes in a network being found together due to random chance. A network score of 2 or greater gives a 99% confidence the network and genes not being generated by random chance alone.

[3] Genes are differentially regulated in metritis cows.

Table 3.

Predicted upstream regulators of differentially expressed genes.

Upstream regulator	Predicted activation state	Z-score	Differentially expressed target molecules
NFκB (complex)	Activated	2.908	*CALB1, CDX1, F3, HGFAC, IL18, LHCGR, NCF2, PLA2G2A, SLC2A4, SOX5, TRIB3, VSNL1*
TCF7L2	Activated	2.414	*CAP1, GCG, ID4, PRICKLE1, TRIM59, UGT8*
IL21	Activated	2.407	*CD28, GZMA, KLRC1, KLRD1, KLRK1, NCR1*
E. coli B5 lipopolysaccharide	Activated	2.219	*F3, IL18, MAT1A, NCF2, TTR*
ITK	Activated	2.219	*KLRC1, KLRD1, KLRK1, NCR1, PRKCB*
NEUROG3	Activated	2.2	*CHGA, EN1, GCG, PPY, SST*
IL12 (complex)	Activated	2.176	*CD28, GZMA, IL18, KLRC1, KLRD1, NCR1*
RAS	Activated	2	*ARHGEF2, CDKN2B, CDX1, GCG*
FGF1	Inhibited	−2.236	*EN1, NDNF, NR4A2, PRICKLE1, TTR*
methylprednisolone	Inhibited	−2.216	*ALDOB, AQP8, C9, F3, HSD17B2, PCTP*
cycloheximide	Inhibited	−2.213	*ADCYAP1, GCG, NR4A1, PLA2G2A, SST*
HES1	Inhibited	−2	*ATOH1, CHGA, GCG, SST*